© 2007 The Chemical Society of Japan

Control of Coordination and Luminescence Properties of Lanthanide Complexes Using Octadentate Oligopyridine-Amine Ligands

Atsushi Wada,[1] Masayuki Watanabe,[1,2] Yoshinori Yamanoi,[1] Takuya Nankawa,[2] Kosuke Namiki,[1] Mikio Yamasaki,[3] Masaki Murata,[1] and Hiroshi Nishihara*[1]

[1]Department of Chemistry, School of Science, The University of Tokyo, 7-3-1 Hongo, Bunkyo-ku, Tokyo 113-0033

[2]Department of Materials Science, Japan Atomic Energy Agency, Tokai-mura, Ibaraki 319-1195

[3]Rigaku Corporation, 3-9-12 Matsubara-cho, Akishima, Tokyo 196-8666

Received May 22, 2006; E-mail: nisihara@chem.s.u-tokyo.ac.jp

Lanthanide complexes with linear and cyclic octadentate oligopyridine-amine ligands were synthesized, and their molecular structures were determined by single-crystal X-ray crystallography. All of the complexes had a distorted capped square antiprism (CSAP) geometry, and the coordination environments of lanthanide complexes were more distorted for the complexes with the linear ligand than those with the cyclic ligand. The Eu^{3+} and Tb^{3+} complexes showed intense luminescence due to energy transfer from the ligand to the metal center (antenna effect). The Eu^{3+} complexes with the linear ligand showed more intense emissions, which were attributed to the $^5D_0 \rightarrow {}^7F_2$ transition, than the complex with the cyclic ligand in acetonitrile, which can be attributed to the distortion in the coordination environments. In contrast, the coordination of water molecules to Eu^{3+} and Tb^{3+} ions was strongly prevented because the metal ions were surrounded by the cyclic ligand, resulting in intense luminescence in water. These results indicate that the coordination environments of lanthanide complexes, and thus the luminescence properties, can be controlled by tuning the geometrical structures of polydentate ligands.

In the last two decades, there has been rapid growth in the field of the coordination chemistry of lanthanides; in particular, luminescent lanthanide complexes have attracted much attention with regard to a variety of optical applications, including as chromophores for LEDs (light-emitting diodes) and as biological labels and sensors.[1–8] Lanthanide ions have intriguing luminescence properties, including millisecond lifetimes and sharp emission bands, and the excitation of the ions by energy transfer from organic ligands causes more intense luminescence (antenna effect) than the direct excitation of f–f transition bands because their molar decadic absorption coefficients (ε)[9] are extremely low. To achieve this antenna effect more effectively, ligands must contain a transition band with a large ε that will populate the excited states.[10–13]

The luminescence from f–f transitions is affected by the symmetry around a lanthanide ion.[11,14–16] In the Judd–Ofelt theory, the symmetry determines the radiative transition probabilities.[17,18] There has been some research on the control of this symmetry to improve luminescence properties based on this theory. Tanabe et al. have reported that the luminescence properties of lanthanide ions improve when they are used to dope asymmetric glasses.[19] Ziessel et al. have reported that the quantum yields of lanthanide complexes change according to the counter ion, which induces a change in the structures of the complexes.[20]

In order to use lanthanide complexes as biological labels and sensors, it is important that they exhibit intense luminescence in water. A general strategy is to synthesize ligands that encapsulate the lanthanide ion completely to prevent the coordination of water molecules that would quench the luminescence.[2,10–12] For example, cryptand-type ligand containing three 2,2′-bipyridine units creates the cavity, in which the lanthanide ion resides ([Ln⊂bpy. bpy. bpy]$^{3+}$) and which protects it against the coordination of water molecules.[21–23]

We have contemplated controlling the coordination environments of lanthanide complexes using octadentate oligopyridine-amine ligands based on a linear or cyclic backbone structure (see Scheme 1). The rigid ligand **1** with a cyclic backbone structure should coordinate more symmetrically than the flexible ligand **2** with a linear backbone structure. Ligand **3** was expected to coordinate less symmetrically than **2**, because the complex with **3** forms two six-membered rings between the lanthanide ion and the backbone structure. In this paper, we report the syntheses, structures, and luminescence properties of lanthanide complexes with a linear or cyclic octadentate oligopyridine-amine ligand. The effects of the coordination environments of lanthanide complexes induced by the ligand backbone structure on the luminescence properties of their Eu^{3+} and Tb^{3+} complexes are described.

Results and Discussion

Syntheses. A cyclic oligopyridine-amine ligand combined with Na^+ and Cl^- ions **4** was synthesized via the method reported in the literature.[24] The free ligand **1** was synthesized from **4** by washing thoroughly with H_2O to remove Na^+ and Cl^- ions. Linear oligopyridine-amine ligands **2** and **3** were newly synthesized in one step from 2-(chloromethyl)pyridine hydrochloride and the corresponding amine in water by maintaining the pH of the reaction mixture between 7 and 9. The products were extracted with diethyl ether and then purified

Published on the web February 13, 2007; doi:10.1246/bcsj.80.335

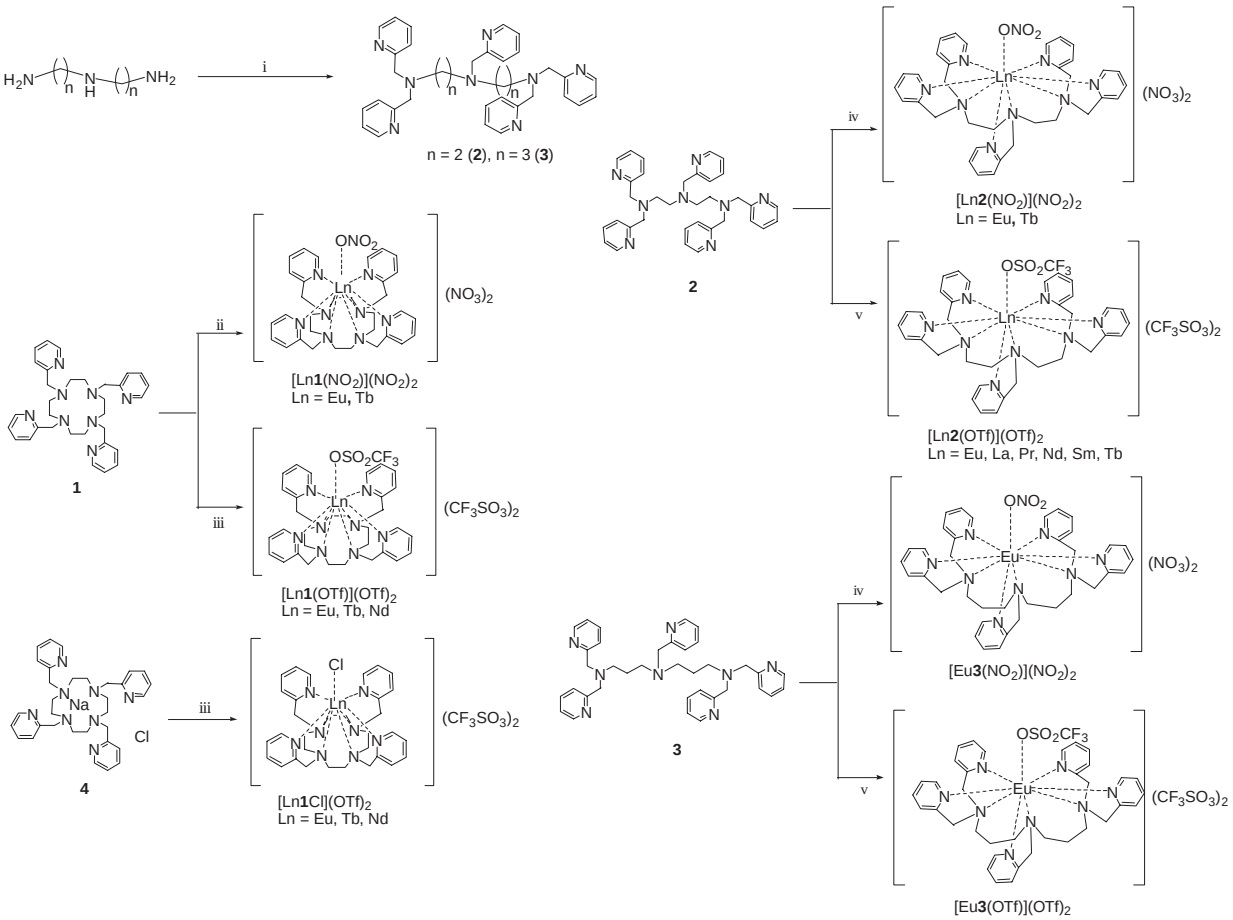

Scheme 1. Synthesis of octadentate oligopyridine-amine ligands and their lanthanide complexes. Conditions: (i) 2-(chloromethyl)-pyridine, 4 mol dm^{-3} NaOH aq (dropwise), H_2O, room temperature, pH 7–9; (ii) $Ln(NO_3)_3 \cdot 6H_2O$, CH_3CN, reflux; (iii) $Ln(OTf)_3$, CH_3CN, reflux; (iv) $Ln(NO_3)_3 \cdot 6H_2O$, CH_3CN, room temperature; (v) $Ln(OTf)_3$, CH_3CN, room temperature.

via column chromatography using basic alumina and preparative HPLC with an ODS column.

Lanthanide complexes of **1** and **2** with triflate ions or a chloride ion were obtained in moderate yields (54–75%) by the reaction of $Eu(OTf)_3$, $Tb(OTf)_3$, and $Nd(OTf)_3$ with one equivalent of **1**, **2**, or **4** in acetonitrile. The Eu^{3+} and Tb^{3+} complexes of **1** and **2** with nitrate ions were also prepared using $Eu(NO_3)_3$ and $Tb(NO_3)_3$, respectively, as a starting material. Elemental analysis, single-crystal X-ray structural analysis, and IR spectra of the products indicate that all the lanthanide complexes have the same formula [Ln**1**Cl](OTf)$_2$, [Ln**1**(OTf)](OTf)$_2$, [Ln**2**(OTf)](OTf)$_2$, or [Ln**1**(NO$_3$)](NO$_3$)$_2$, where the lanthanide metal is coordinated by eight nitrogen atoms of **1** or **2** and a chlorine atom or an oxygen atom (vide infra). The crystal structures of lanthanide complexes of **2** with nitrate ions have not been determined, but the NO stretching vibrations in the IR spectra gave information on the coordination of the nitrate ions, as the NO stretching vibration of free NO appears at 1380 cm^{-1} and that of coordinating NO at 1470 and 1300 cm^{-1}.[25,26] A sharp peak appeared at 1384 cm^{-1} for free nitrate, and also two intense peaks at 1476 and 1300 cm^{-1} for coordinating nitrate in the Eu complex of **2**, indicating a structure of [Eu**2**(NO$_3$)](NO$_3$)$_2$, in which a nitrate ion acts as an O-coordinating monodentate ligand like in [Eu**1**-(NO$_3$)](NO$_3$)$_2$.[27] Similarly, the Tb complex of **2**, which had similar peaks (1384 cm^{-1} for free nitrate and at 1482 and 1296 cm^{-1} for a coordinating nitrate), is nine-coordinate and can be written as [Tb**2**(NO$_3$)](NO$_3$)$_2$ (Fig. S1 of Supporting Information).

The Eu complexes of **3** with three triflate or nitrate ions were also prepared in the same manner as that for the complexes of **1** and **2** as noted above. Their crystal structures have not been determined, but it is likely that they have a similar nine-coordinate structure, [Eu**3**(OTf)](OTf)$_2$ and [Eu**3**(NO$_3$)]-(NO$_3$)$_2$, based on the comparison of its IR spectra with those of the complexes of **1** and **2**.

Crystal Structures. Single crystals of [Nd**1**Cl](OTf)$_2$, [Eu**1**Cl](OTf)$_2$, [Tb**1**Cl](OTf)$_2$, [Nd**1**(OTf)](OTf)$_2$, [Eu**1**-(OTf)](OTf)$_2$, [Eu**1**(NO$_3$)](NO$_3$)$_2$, [La**2**(OTf)](OTf)$_2$, [Pr**2**-(OTf)](OTf)$_2$, [Nd**2**(OTf)](OTf)$_2$, [Sm**2**(OTf)](OTf)$_2$, and [Eu**2**(OTf)](OTf)$_2$ were obtained by recrystallization from dichloromethane/ethyl acetate or from acetonitrile/diethyl ether, and their structures were determined by X-ray structural analysis. Crystallographic data thus obtained are summarized in Table 1.

Figure 1A displays an ORTEP drawing of [Eu**1**Cl](OTf)$_2$, where Eu^{III} is bound to eight nitrogen atoms of **1** and one chloride ion. Molecular structures of [Nd**1**Cl](OTf)$_2$ and [Tb**1**Cl]-(OTf)$_2$ are similar to the structure of [Eu**1**Cl](OTf)$_2$ (see Figs. S2 and S3, Supporting Information). The geometry of

Table 1. Crystallographic Data for the Lanthanide Complexes of Oligopyridine-Amine Ligands

	[Nd**1**Cl](OTf)$_2$	[Eu**1**Cl](OTf)$_2$	[Tb**1**Cl](OTf)$_2$	[Nd**1**(OTf)](OTf)$_2$·2MeCN·0.5Et$_2$O	[Eu**1**(OTf)](OTf)$_2$·2MeCN	[Eu**1**(NO$_3$)](NO$_3$)$_2$·2MeCN	[La**2**(OTf)](OTf)$_2$·2CH$_2$Cl$_2$	[Pr**2**(OTf)](OTf)$_2$	[Nd**2**(OTf)](OTf)$_2$	[Sm**2**(OTf)](OTf)$_2$	[Eu**2**(OTf)](OTf)$_2$·2CH$_2$Cl$_2$
Formula	$C_{34}H_{40}ClF_6$-$N_8NdO_6S_2$	$C_{34}H_{40}ClEuF_6$-$N_8O_6S_2$	$C_{34}H_{40}ClF_6$-$N_8O_6S_2Tb$	$C_{41}H_{51}F_9$-$N_{10}NdO_{9.5}S_3$	$C_{39}H_{46}EuF_9$-$N_{10}O_9S_3$	$C_{36}H_{46}EuF_9$-$N_{13}O_9$	$C_{39}H_{42}Cl_4F_9La$-$N_8O_9S_3$	$C_{37}H_{38}F_9$-$N_8O_9PrS_3$	$C_{37}H_{38}F_9$-$N_8NdO_9S_3$	$C_{37}H_{38}F_9$-$N_8O_9S_3Sm$	$C_{39}H_{42}Cl_4EuF_9$-$N_8O_9S_3$
mol wt	1014.5	1022.3	1029.2	1247.3	1218.0	1127.8	1314.7	1146.8	1150.2	1156.3	1327.8
Crystal system	orthorhombic	orthorhombic	orthorhombic	orthorhombic	orthorhombic	monoclinic	monoclinic	monoclinic	monoclinic	monoclinic	monoclinic
Space group	$P22_12_1$	$P22_12_1$	$P22_12$	$Pbcn$	$Pbna$	$P2_1/c$	$P2_1$	$P2_1$	$P2_1$	$P2_1$	$P2_1$
a/Å	8.414(5)	8.346(2)	8.325(2)	34.156(4)	13.372(2)	31.468(1)	12.129(5)	12.4803(11)	12.254(5)	12.4563(19)	12.453(2)
b/Å	11.049(5)	11.116(3)	11.113(1)	13.370(2)	21.924(4)	10.876(4)	11.942(5)	11.7477(5)	11.843(5)	11.7230(11)	11.686(2)
c/Å	21.470(5)	21.206(5)	21.4630(7)	21.919(3)	33.927(6)	37.931(1)	18.174(1)	17.9642(13)	18.092(7)	17.975(2)	17.919(4)
α/deg	90	90	90	90	90	90	90	90	90	90	90
β/deg	90	90	90	90	90	113.619(5)	104.386(5)	102.8910(10)	103.425(2)	102.827(2)	102.656(3)
γ/deg	90	90	90	90	90	90	90	90	90	90	90
V/Å^3	1996.0(16)	1967.2(8)	1985.7(6)	10010(2)	9946(3)	11894(6)	2549.9(17)	2567.4(3)	2553.8(18)	2559.3(6)	2544.3(8)
Z	2	2	2	8	8	12	2	2	2	2	2
GOF	1.081	1.106	1.232	1.116	1.13	1.199	1.031	1.062	1.076	1.057	1.042
R_1[a)]	0.0491	0.0547	0.1101	0.0618	0.1001	0.1551	0.0470	0.0914	0.0660	0.0893	0.0773
wR_2[b)]	0.1356	0.1361	0.2647	0.1424	0.255	0.37	0.1185	0.2589	0.2011	0.2564	0.2033

a) $R_1 = \sum ||F_o| - |F_c|| / \sum |F_o|$ ($I > 2\sigma(I)$). b) $wR_2 = [\sum w(|F_o^2| - |F_c^2|)^2 / \sum w|F_o^2|^2]^{1/2}$ ($I > 2\sigma(I)$).

nine-coordinate complexes predominantly involved a tricapped trigonal prism (TTP) or capped square antiprism (CSAP). The distinguishing features of these two geometries are the dihedral angle between trigonal faces (N1, N4, N5) and (N2, N3, N7), which is 180° for idealized TTP and 163.5° for idealized CSAP, and the dihedral angle between trigonal faces (N6, N7, N5) and (N8, N7, N5), which is 26.4° for idealized TTP and 0° for idealized CSAP. For [Nd**1**Cl](OTf)$_2$, [Eu**1**Cl](OTf)$_2$, and [Tb**1**Cl](OTf)$_2$, the former angles were 166.2, 163.9, and 164.4°, and the latter ones were 0, 0.2, and 0.1° (Table 2), indicating that the geometry for [Nd**1**Cl](OTf)$_2$, [Eu**1**Cl](OTf)$_2$, and [Tb**1**Cl](OTf)$_2$ is distorted CSAP.[28–30] Four pyridine nitrogen atoms (N1, N2, N3, and N4) form one basal plane, four amine nitrogen atoms (N5, N6, N7, and N8) occupy the second plane, and a chloride ion acts as a cap above the planes.

An ORTEP drawing of [Eu**1**(OTf)](OTf)$_2$ and [Eu**1**(NO$_3$)](NO$_3$)$_2$ are shown in Figs. 1B and 1C, respectively, where the coordination number of the Eu^{III} center is also 9, with eight nitrogen atoms of **1** and one oxygen atom of a triflate or nitrate ion as coordinating atoms. The molecular structure of [Nd**1**(OTf)](OTf)$_2$ is similar to the structure of [Eu**1**(OTf)](OTf)$_2$ (see Fig. S4, Supporting Information). The dihedral angle between (N1, N4, N5) and (N2, N3, N7) were 169.4, 168.9, and 169.1°, and that between (N6, N7, N5) and (N8, N7, N5) were 0.7, 0.9, and 0.1° for [Nd**1**(OTf)](OTf)$_2$, [Eu**1**(OTf)](OTf)$_2$, and [Eu**1**(NO$_3$)](NO$_3$)$_2$, respectively (Table 2), indicating that the geometry was also distorted CSAP.[28–30] Similar to [Eu**1**Cl](OTf)$_2$, four pyridine nitrogen atoms and four amine nitrogen atoms formed two planes, and one oxygen atom of a triflate or nitrate ion is capped above the planes.

The selected bond lengths and angles for [Eu**1**Cl](OTf)$_2$, [Eu**1**(OTf)](OTf)$_2$, and [Eu**1**(NO$_3$)](NO$_3$)$_2$ are summarized in Table 3, and the Ln–N bond lengths are shown in Fig. 2. The Eu–N bond lengths for [Eu**1**Cl](OTf)$_2$, [Eu**1**(OTf)](OTf)$_2$, and [Eu**1**(NO$_3$)](NO$_3$)$_2$ were 2.596(6)–2.652(5), 2.591(8)–2.646(8), and 2.568(14)–2.644(14) Å, respectively, which are typical values and are within a narrow range; the ranges of the Eu–N bond lengths reported for the Eu complexes with N-donor ligand(s) are 2.599(3)–2.658(3) Å for [Eu(*p*-MOBA)$_3$bipy]·1/2C$_2$H$_5$OH (*p*-MOBA = 4-methoxybenzene and bipy = 2,2′-bipyridine), 2.593(3)–2.658(3) Å for [Eu(*o*-ABA)$_3$bipy]bipy (*o*-ABA = *o*-aminobenzoate), 2.616(5)–2.625(5) Å for [Eu(HFAA)$_3$bipy·H$_2$O] (HFAA = hexafluoroacetylacetone), 2.540(5)–2.554(5) Å for [Eu(bipy)$_2$(NO$_3$)$_3$], 2.538(4)–2.574(4) Å for [Eu(terpy)(NO$_3$)$_3$·H$_2$O], 2.597(4)–2.609(4) Å for [Eu(ODA)phen·4H$_2$O]Cl·5H$_2$O (ODA = oxydiacetate, phen = 1,10-phenanthroline), 2.572(9)–2.623(9) Å for [Eu(*m*-BrBA)$_3$phen·H$_2$O]$_2$ (*m*-BrBA = *m*-bromobenzoate), 2.556(4)–2.624(4) Å for [Eu$_2$(SA)$_6$(phen)$_2$]·6H$_2$O and [Eu$_2$(SA)$_4$(phen)$_2$(H$_2$O)$_4$](ClO$_4$)$_3$(phenH)·H$_2$O (SA = succinamate), 2.592(6) Å for [Eu(DPAP)$_3$]·12H$_2$O (DPAP = 6-diphenylcarbamoyl-2-pyridinecarboxylato), 2.579(9)–2.683(7) Å for Na[Eu(TETA)]·2H$_2$O·4NaCl (TETA = 1,4,8,11-tetraazacyclotetradecane-1,4,8,11-tetraacetate), 2.568(3)–2.649(3) Å for [Eu(CH$_3$CO$_2$)$_2$(C$_{22}$H$_{26}$N$_6$)](CH$_3$CO$_2$)·9H$_2$O, 2.522(3)–2.730(3) Å for [Eu(tpa)$_2$](OTf)$_3$, [Eu(tpa)(OTf)$_3$(H$_2$O)$_2$]$_3$ and [Eu(tpa)(*u*-OH)(OTf)$_2$]$_2$ (tpa = tris(2-pyridylmethyl)amine) and 2.6757(16)–2.7085(17) Å for [Eu(DBM)$_3$(TPTZ)](C$_3$H$_6$O) (DBM = dibenzoylmethanate, TPTZ = 2,4,6-tri(2-pyrydyl)-

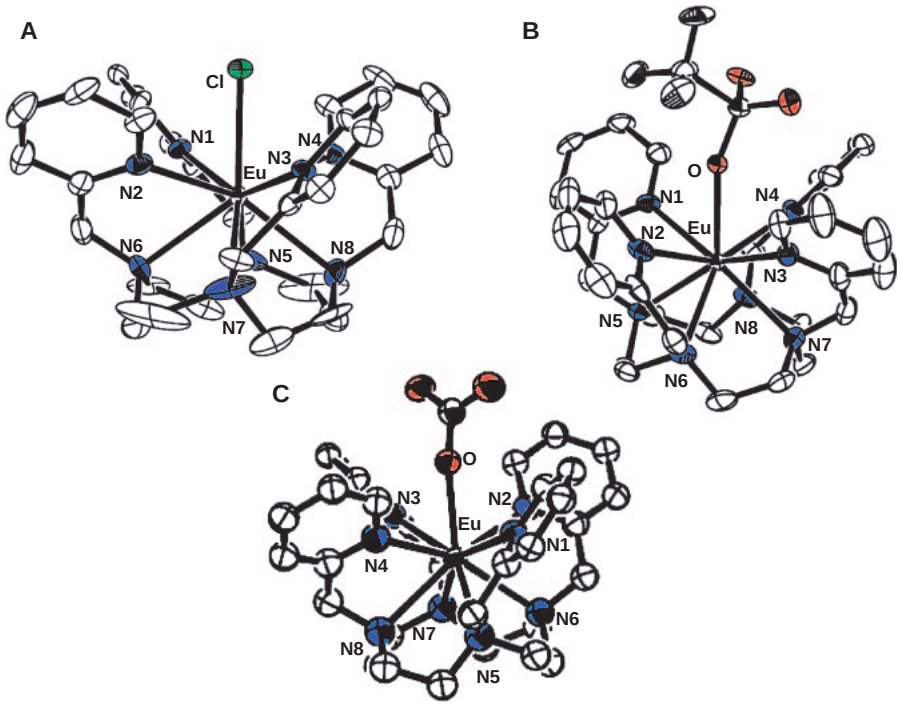

Fig. 1. ORTEP drawings of [Eu**1**Cl](OTf)$_2$ (**A**), [Eu**1**(OTf)](OTf)$_2$ (**B**), and [Eu**1**(NO$_3$)](NO$_3$)$_2$ (**C**) with 50% probability. H atoms, solvent molecules, triflates and nitrates except for those that are coordinating have been omitted for clarity.

Table 2. Selected Dihedral Angles

Complex	(N1, N4, N5)–(N2, N3, N7) /deg	(N6, N7, N5)–(N8, N7, N5) /deg
Idealized TTP	180.0	26.4
[Nd**1**Cl](OTf)$_2$	166.2	0.0
[Eu**1**Cl](OTf)$_2$	163.9	0.2
[Tb**1**Cl](OTf)$_2$	164.4	0.1
[Nd**1**(OTf)](OTf)$_2$	169.4	0.7
[Eu**1**(OTf)](OTf)$_2$	168.9	0.9
[Eu**1**(NO$_3$)](NO$_3$)$_2$	169.1	0.1
[La**2**(OTf)](OTf)$_2$	155.5	0.5
[Pr**2**(OTf)](OTf)$_2$	152.4	1.3
[Nd**2**(OTf)](OTf)$_2$	154.5	0.6
[Sm**2**(OTf)](OTf)$_2$	151.9	1.4
[Eu**2**(OTf)](OTf)$_2$	152.4	1.1
Idealized CSAP	163.5	0.0

1,3,5-triazine).[31–42] The N(pyridine)–Eu–N(pyridine) and the N(amine)–Eu–N(amine) angles are within a narrow range from 82.5(2) to 86.7(2)° and from 67.7(4) to 68.3(5)° for [Eu**1**Cl](OTf)$_2$, from 81.9(3) to 87.0(3)° and from 66.9(3) to 67.9(3)° for [Eu**1**(OTf)](OTf)$_2$ and from 82.7(4) to 84.6(3)° and from 66.7(4) to 67.8(4)° for [Eu**1**(NO$_3$)](NO$_3$)$_2$, respectively. Consequently, all the Eu complexes of **1** are relatively symmetrical and have a pseudo-C_4 rotation axis.

An ORTEP drawing of [Eu**2**(OTf)](OTf)$_2$ is shown in Fig. 3. The molecular structures of [La**2**(OTf)](OTf)$_2$, [Pr**2**(OTf)](OTf)$_2$, [Nd**2**(OTf)](OTf)$_2$, and [Sm**2**(OTf)](OTf)$_2$ are similar to the structure of [Eu**2**(OTf)](OTf)$_2$ (see Figs. S5, S6, S7, and S8, Supporting Information). The coordination number of the Ln^{III} (Ln = La, Pr, Nd, Sm, and Eu) is 9; all

Table 3. Selected Bond Lengths (Å) and Angles (deg) for [Eu**1**Cl](OTf)$_2$, [Eu**1**(OTf)](OTf)$_2$, and [Eu**1**(NO$_3$)](NO$_3$)$_2$

	[Eu**1**Cl](OTf)$_2$	[Eu**1**(OTf)](OTf)$_2$	[Eu**1**(NO$_3$)](NO$_3$)$_2$
Eu–N1 (pyridine)	2.626(6)	2.628(8)	2.570(13)
Eu–N2 (pyridine)	2.596(6)	2.599(8)	2.568(14)
Eu–N3 (pyridine)	2.626(6)	2.591(8)	2.590(14)
Eu–N4 (pyridine)	2.596(6)	2.597(8)	2.574(13)
Eu–N5 (amine)	2.652(6)	2.640(8)	2.641(14)
Eu–N6 (amine)	2.627(6)	2.646(8)	2.644(14)
Eu–N7 (amine)	2.652(6)	2.643(8)	2.641(14)
Eu–N8 (amine)	2.627(6)	2.617(8)	2.638(13)
Eu–X (X = Cl and O)	2.725(2)	2.508(6)	2.430(12)
N1–Eu–N2	82.5(2)	82.2(3)	84.2(4)
N2–Eu–N3	86.7(2)	83.6(3)	82.7(4)
N3–Eu–N4	82.5(2)	81.9(3)	83.1(4)
N4–Eu–N1	86.7(2)	87.0(3)	84.6(4)
N5–Eu–N6	68.3(5)	66.9(3)	67.1(4)
N6–Eu–N7	67.7(4)	67.3(3)	66.7(4)
N7–Eu–N8	68.3(5)	67.6(3)	67.8(4)
N8–Eu–N5	67.7(4)	67.9(3)	67.1(4)

of the nitrogen atoms of **2** and one oxygen atom from a triflate ion are coordinated. Values of the dihedral angle between (N1, N4, N5) and (N2, N3, N7) were 155.5, 152.4, 154.5, 151.9, and 152.4°, and those of the dihedral angle between (N6, N7, N5) and (N8, N7, N5) were 0.5, 1.3, 0.6, 1.4, and 1.1°, for the La, Pr, Nd, Sm, and Eu complexes, respectively. These findings indicate that the geometry of each complex is also distorted CSAP (Table 2).[28–30] Four pyridine nitrogen atoms (N1, N2, N3, and N4) form one basal plane, one pyridine nitrogen

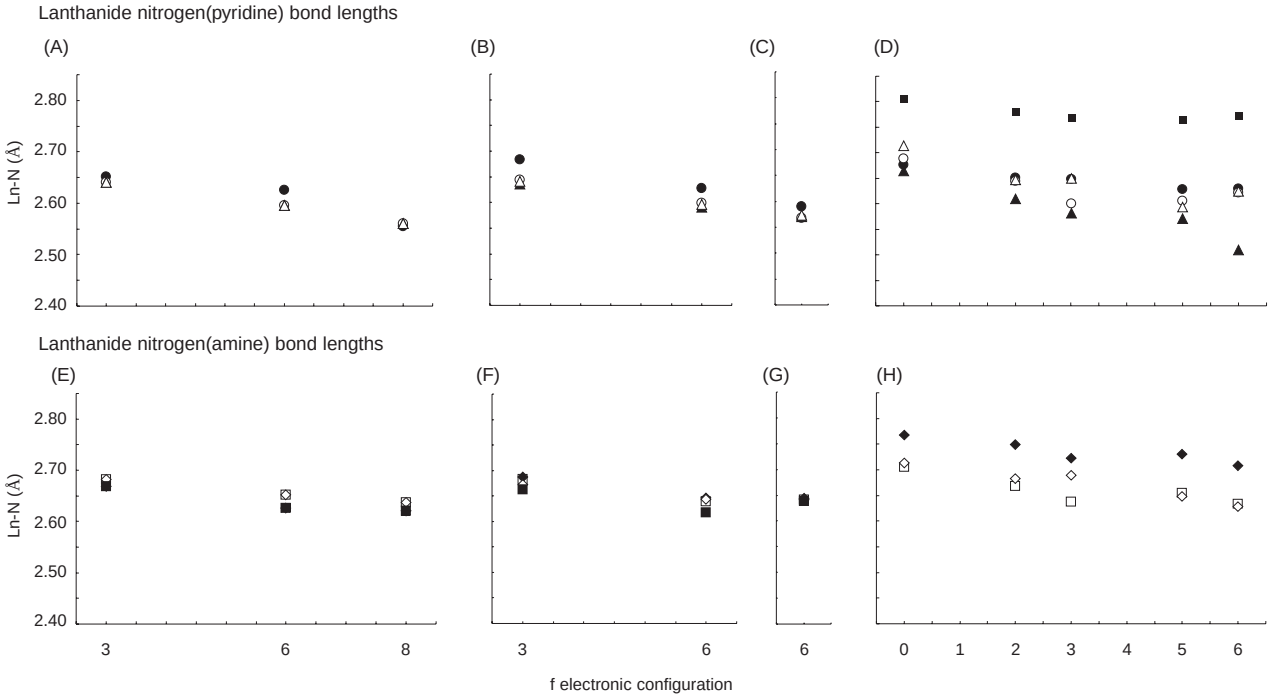

Fig. 2. Lanthanide(III) nitrogen bond lengths (Å) vs f electronic configuration in [Ln**1**Cl](OTf)$_2$ (Ln = Nd, Eu, and Tb) (A and E), [Ln**1**(OTf)](OTf)$_2$ (Ln = Nd and Eu) (B and F), [Eu**1**(NO$_3$)](NO$_3$)$_2$ (C and G), and [Ln**2**(OTf)](OTf)$_2$ (Ln = La, Pr, Nd, Sm, and Eu) (D and H); ●: Ln–N1, ○: Ln–N2, ▲: Ln–N3, △: Ln–N4, ■: Ln–N5, □: Ln–N6, ◆: Ln–N7, ◇: Ln–N8.

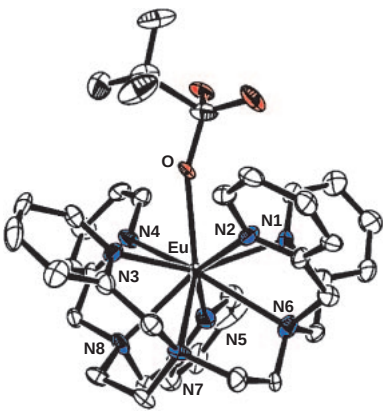

Fig. 3. ORTEP drawing of [Eu**2**(OTf)](OTf)$_2$ with 50% probability. H atoms, solvent molecules, and triflates except for those that are coordinating have been omitted for clarity.

(N5) and three amine nitrogen atoms (N6, N7, N8) form the second plane and an oxygen atom from the triflate ion acts as a cap above the planes.

The Ln–N bond lengths for [La**2**(OTf)](OTf)$_2$, [Pr**2**(OTf)](OTf)$_2$, [Nd**2**(OTf)](OTf)$_2$, [Sm**2**(OTf)](OTf)$_2$, and [Eu**2**(OTf)](OTf)$_2$ are plotted against the number of f-electrons in Fig. 2 (and Table S1 of Supporting Information). The bond lengths decreased as the number of the f-electrons increased. The decreases in the Ln–N8 bond length from La^{3+} to Pr^{3+}, from La^{3+} to Sm^{3+}, and from La^{3+} to Eu^{3+} were 0.03, 0.07, and 0.09 Å, respectively, which are in agreement with the differences in the ionic radii calculated from Shannon's ionic radii for nona-coordinated ions.[43]

Table 4. Selected Bond Lengths (Å) and Angles (deg) for [Eu**2**(OTf)](OTf)$_2$

Eu–N1 (pyridine)	2.630(11)	N1–Eu–N2	82.8(3)
Eu–N2 (pyridine)	2.621(10)	N2–Eu–N3	78.8(3)
Eu–N3 (pyridine)	2.509(11)	N3–Eu–N4	83.4(3)
Eu–N4 (pyridine)	2.624(11)	N4–Eu–N1	97.6(3)
Eu–N5 (pyridine)	2.774(10)	N5–Eu–N6	84.0(3)
Eu–N6 (amine)	2.633(11)	N6–Eu–N7	67.7(4)
Eu–N7 (amine)	2.708(7)	N7–Eu–N8	66.3(4)
Eu–N8 (amine)	2.628(11)	N8–Eu–N5	64.2(3)
Eu–O	2.445(6)		

The selected bond lengths and angles for [Eu**2**(OTf)](OTf)$_2$ are summarized in Table 4. The Eu–N1–4 and Eu–N6–8 bond lengths were 2.509(11)–2.708(7) Å, which are within the range of reported values for the Eu complexes with N-donor ligands, while the Eu–N5 (2.774(10) Å) bond lengths were out of this range.[31–42] The N(pyridine)–Eu–N(pyridine) and N(amine)–Eu–N(amine) angles ranged between 64.2(3) and 97.6(3)°. These results imply that [Eu**2**(OTf)](OTf)$_2$ is less symmetrical than [Eu**1**Cl](OTf)$_2$, [Eu**1**(OTf)](OTf)$_2$, and [Eu**1**(NO$_3$)](NO$_3$)$_2$.

Schematic drawings of [Eu**1**(OTf)](OTf)$_2$ and [Eu**2**(OTf)](OTf)$_2$ are shown in Fig. 4. The distances between N1 and N5 (3.08(3) Å) and between N5 and N6 (3.62(3) Å) for [Eu**2**(OTf)](OTf)$_2$ are much longer than those for [Eu**1**(OTf)](OTf)$_2$ (2.72(17) and 2.913(13) Å) by 0.36(17) and 0.71(3) Å, respectively, while the differences of the other N–N distances between the two complexes were within 0.16(17) Å. The N5 atom of [Eu**2**(OTf)](OTf)$_2$ was far from the ideal position in the CSAP geometry because the Eu^{3+} ion is too large to be

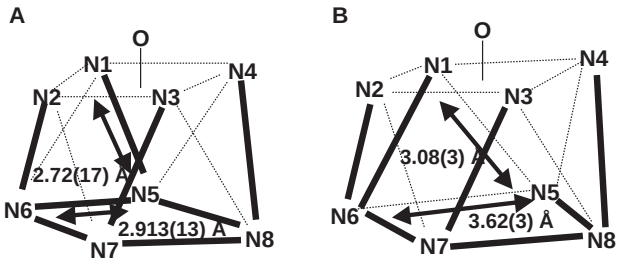

Fig. 4. Schematic drawings of [Eu**1**(OTf)](OTf)$_2$ (**A**) and [Eu**2**(OTf)](OTf)$_2$ (**B**).

completely encapsulated by the ligands. It can be concluded that a flexible linear ligand **2** forms a more distorted complex than a rigid cyclic ligand **1** does.

Photoluminescence Properties. The UV, excitation and emission spectra of [Eu**2**(NO$_3$)](NO$_3$)$_2$ and [Tb**2**(NO$_3$)](NO$_3$)$_2$ are shown in Fig. 5. The emission spectrum for [Eu**2**-(NO$_3$)](NO$_3$)$_2$ had characteristic sharp emission bands at 594 nm ($^5D_0 \rightarrow {}^7F_1$), 618 nm ($^5D_0 \rightarrow {}^7F_2$), 650 nm ($^5D_0 \rightarrow {}^7F_3$), and 693 nm ($^5D_0 \rightarrow {}^7F_4$). The emission bands for [Tb**2**(NO$_3$)](NO$_3$)$_2$ appeared at 491 nm ($^5D_4 \rightarrow {}^7F_6$), 545 nm ($^5D_4 \rightarrow {}^7F_5$), 586 nm ($^5D_4 \rightarrow {}^7F_4$), and 622 nm ($^5D_4 \rightarrow {}^7F_3$). The excitation spectra corresponded to the absorption spectra of the ligands throughout the UV region, con-

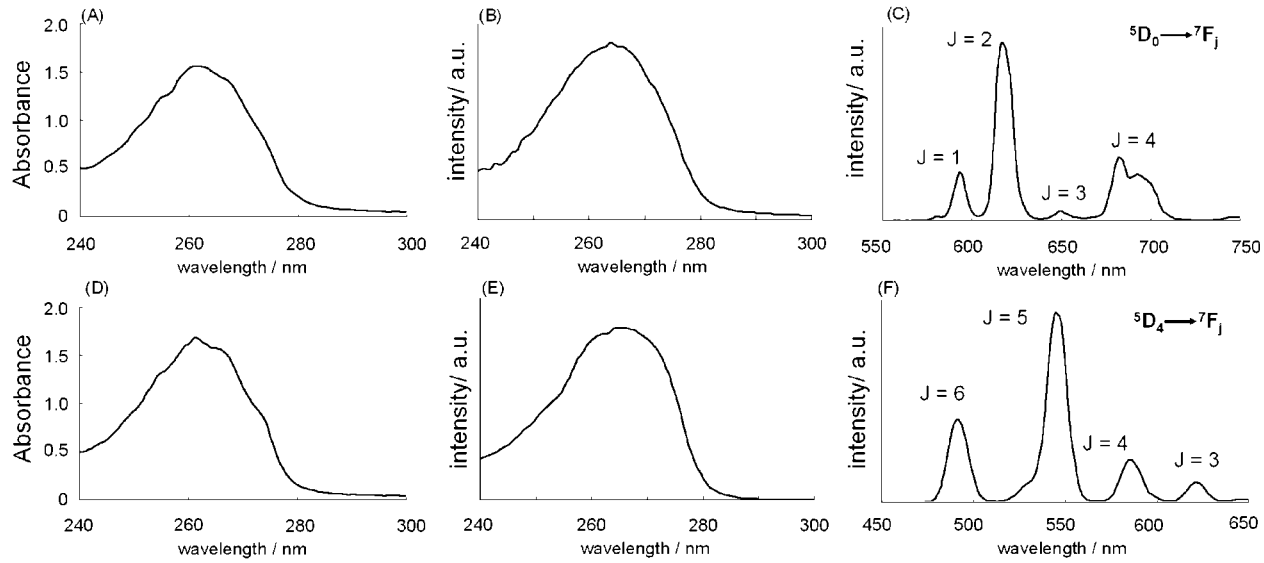

Fig. 5. UV, excitation and emission spectra of [Eu**2**(NO$_3$)](NO$_3$)$_2$ (A, B, and C) and [Tb**2**(NO$_3$)](NO$_3$)$_2$ (D, E, and F) in CH$_3$CN at room temperature. The emission and excitation wavelength for [Eu**2**(NO$_3$)](NO$_3$)$_2$ are 618 and 263 nm and those for [Tb**2**(NO$_3$)]-(NO$_3$)$_2$ are 545 and 265 nm, respectively. The concentration of [Eu**2**(NO$_3$)](NO$_3$)$_2$ and [Tb**2**(NO$_3$)](NO$_3$)$_2$ is 1.0×10^{-4} mol dm^{-3}. Intensity maxima for [Eu**2**(NO$_3$)](NO$_3$)$_2$ and [Tb**2**(NO$_3$)](NO$_3$)$_2$ are 618 and 545 nm, respectively.

Table 5. Absorption and Luminescence Properties of the Eu^{3+} and Tb^{3+} Complexes

	Absorption[a]		Quantum yield[c]		Lifetime[d]
	λ_{max}/nm	ε_{max}/mol^{-1} dm^3 cm^{-1}	Φ_{CH_3CN}[a]	Φ_{H_2O}[b]	τ_{CH_3CN}/ms
[Eu**1**(NO$_3$)](NO$_3$)$_2$	267	11000	0.016	0.012	0.75
[Eu**1**(OTf)](OTf)$_2$	268	11400	0.015	0.013	0.87
[Eu**1**Cl](OTf)$_2$	263	12000	0.024	0.016	1.10
[Eu**2**(NO$_3$)](NO$_3$)$_2$	262	15900	0.010	0.005	0.64
[Eu**2**(OTf)](OTf)$_2$	261	15100	0.009	0.004	0.62
[Eu**3**(NO$_3$)](NO$_3$)$_2$	262	13400	0.005	$<10^{-5}$	0.74
[Eu**3**(OTf)](OTf)$_2$	261	14100	0.002	0.0001	0.71
[Tb**1**(NO$_3$)](NO$_3$)$_2$	266	12800	0.77	0.76	1.83
[Tb**1**(OTf)](OTf)$_2$	267	11900	0.82	0.76	2.86
[Tb**1**Cl](OTf)$_2$	263	11300	0.86	0.72	2.85
[Tb**2**(NO$_3$)](NO$_3$)$_2$	263	16000	0.59	0.001	1.60
[Tb**2**(OTf)](OTf)$_2$	265	17600	0.58	0.002	2.01

a) All measurements were performed in acetonitrile at room temperature (295 K). b) All measurements were performed in water at room temperature. c) Upon excitation in the ligand absorption at 260 nm. Estimated experimental error was 30%. d) Luminescence of $^5D_0 \rightarrow {}^7F_2$ (615 nm) for Eu^{3+} and that of $^5D_4 \rightarrow {}^7F_5$ (543 nm) for Tb^{3+} were measured in acetonitrile at room temperature (295 K) to obtain the lifetime, respectively.

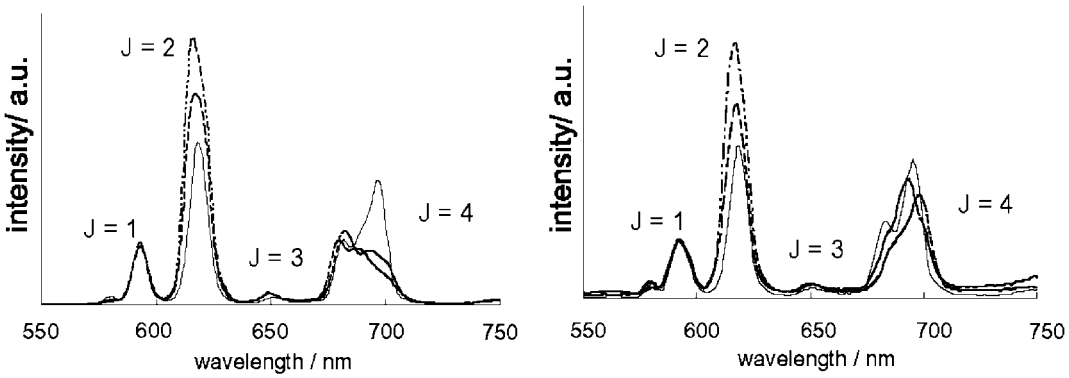

Fig. 6. Emission spectra of the Eu^{3+} complexes (1.0×10^{-4} mol dm^{-3}) normalized with $^5D_0 \rightarrow {}^7F_1$ emission bands at 594 nm in CH_3CN. Left: [Eu**1**(NO_3)]$(NO_3)_2$ (solid line), [Eu**2**(NO_3)]$(NO_3)_2$ (dashed line), [Eu**3**(NO_3)]$(NO_3)_2$ (dash-dot-dot line). Right: [Eu**1**(OTf)](OTf)$_2$ (solid line), [Eu**2**(OTf)](OTf)$_2$ (dashed line), [Eu**3**(OTf)](OTf)$_2$ (dash-dot-dot line).

firming the role of the organic chromophore in sensitizing the Eu^{3+} and Tb^{3+} excited states; in other words, energy transfer from the ligand to a metal center takes places (antenna effect). Similar excitation and emission spectra were observed in other Eu^{3+} and Tb^{3+} complexes with Cl^- and OTf^- ligands.

Absorption and luminescence properties for the Eu^{3+} and Tb^{3+} complexes in acetonitrile and H_2O are summarized in Table 5. The absorption spectra of these complexes are dominated by a $\pi \rightarrow \pi^*$ transition of the pyridine units. As a result of the incorporation of multiple pyridine moieties into the ligand, the molar absorption coefficient values of the Eu^{3+} and Tb^{3+} complexes were high ($\varepsilon_{max} > 10^4\,M^{-1}\,cm^{-1}$). The quantum yield values for the Tb^{3+} complexes of **1** both in acetonitrile and in water had considerably high values: 0.77 and 0.76 for [Tb**1**(NO_3)]$(NO_3)_2$, 0.82 and 0.72 for [Tb**1**(OTf)]-(OTf)$_2$, and 0.86 and 0.72 for [Tb**1**Cl](OTf)$_2$, respectively.

Pertaining to the luminescence of Eu^{3+}, the $^5D_0 \rightarrow {}^7F_1$ transition is magnetic-dipolar in character, and its radiative transition probability is relatively independent of the surroundings of the Eu^{3+} ions. In contrast, the $^5D_0 \rightarrow {}^7F_2$ transition is predominantly electric-dipolar in character, and the emission intensity is very sensitive to the symmetry around the Eu^{3+} ions (hypersensitive transition).[9,13,14] The emission spectra of [Eu**1**(NO_3)]$(NO_3)_2$, [Eu**2**(NO_3)]$(NO_3)_2$, and [Eu**3**(NO_3)]-$(NO_3)_2$, and those of [Eu**1**(OTf)](OTf)$_2$, [Eu**2**(OTf)](OTf)$_2$, and [Eu**3**(OTf)](OTf)$_2$ normalized with respect to the $^5D_0 \rightarrow {}^7F_1$ emission bands, are shown in Fig. 6.[44–47] A comparison of the emission bands due to the $^5D_0 \rightarrow {}^7F_2$ transition shows that the intensity increased in the order [Eu**1**(NO_3)]$(NO_3)_2$ < [Eu**2**(NO_3)]$(NO_3)_2$ < [Eu**3**(NO_3)]$(NO_3)_2$ and [Eu**1**(OTf)]-(OTf)$_2$ < [Eu**2**(OTf)](OTf)$_2$ < [Eu**3**(OTf)](OTf)$_2$. This order is probably due to the distortion in the coordination environments controlled by the backbone structure of the ligands, based on the difference in molecular structure, as described above between the complexes of **1** and those of **2**, whereas the numbers of coordinating amine and pyridine nitrogens are slightly different. It is also reasonable to interpret the order by the effect of the distortion because the complexes of **2** and those of **3** have the same numbers of coordinating amine and pyridine nitrogens, but the intensities of their $^5D_0 \rightarrow {}^7F_2$ emission bands were noticeably different. In other words, the change in the coordination environments induced by the ligand backbone structure brings about an enhancement of the $^5D_0 \rightarrow {}^7F_2$ emission bands in the Eu^{3+} complexes.

The excitation and emission spectra of [Eu**1**(NO_3)]$(NO_3)_2$, [Eu**2**(NO_3)]$(NO_3)_2$, [Eu**3**(NO_3)]$(NO_3)_2$, [Tb**1**(NO_3)]$(NO_3)_2$, and [Tb**2**(NO_3)]$(NO_3)_2$ were measured in H_2O. The emission spectra of [Eu**1**(NO_3)]$(NO_3)_2$, [Eu**2**(NO_3)]$(NO_3)_2$, and [Tb**1**-(NO_3)]$(NO_3)_2$ in acetonitrile and in water are superimposed for comparison in Fig. 7. Intense emissions were observed for [Eu**1**(NO_3)]$(NO_3)_2$ and [Tb**1**(NO_3)]$(NO_3)_2$ even in water, but the emission intensity decreased drastically for [Eu**2**(NO_3)]-$(NO_3)_2$. In addition, no emissions were detected for [Eu**3**-(NO_3)]$(NO_3)_2$ and [Tb**2**(NO_3)]$(NO_3)_2$ in water. These results are likely a consequence of the water-molecule coordination and the ligand dissociation. In order to confirm this hypothesis, we measured the lifetimes of emissions and estimated the number of water molecules coordinated to the metal center (q H_2O) by using Horrocks' equation for the Eu^{3+} complexes and by Parker's equation for the Tb^{3+} complexes.[48,49] The data for the luminescence lifetime and the number of coordinating water thus obtained are summarized in Table 6. The results indicate that three or four water molecules coordinate to the lanthanide ion in [Eu**2**(NO_3)]$(NO_3)_2$, but few water molecules coordinate to [Eu**1**(NO_3)]$(NO_3)_2$ and [Tb**1**(NO_3)]$(NO_3)_2$. In Lehn's cryptate complexes, [Eu⊂bpy. bpy. bpy]$^{3+}$ and [Tb⊂bpy. bpy. bpy]$^{3+}$, the number of coordinated water molecules was 2.5 for [Eu⊂bpy. bpy. bpy]$^{3+}$ and 3.0 for [Tb⊂bpy. bpy. bpy]$^{3+}$, respectively.[21–23] As such, the rigid ligand **1** with a cyclic backbone structure shields the lanthanide ions from water coordination more effectively than the flexible ligand **2** with a linear backbone structure.

Conclusion

We prepared several lanthanide complexes with different coordination environments and showed that the luminescence properties can be controlled by using octadentate oligopyridine-amine ligands with a cyclic backbone **1** and with a linear backbone **2** and **3**. All of lanthanide complexes had a distorted CSAP geometry, but the complex with linear ligand **2** was more distorted than that with cyclic ligand **1**. The Eu^{3+} and Tb^{3+} complexes of **1**–**3** showed intense luminescence due to the antenna effect. The Eu^{3+} complexes with linear ligand **2** or **3** showed more intense $^5D_0 \rightarrow {}^7F_2$ emissions than that with cyclic ligand **1**, which was caused by the distortion in the coordination environments. The ability to protect against water

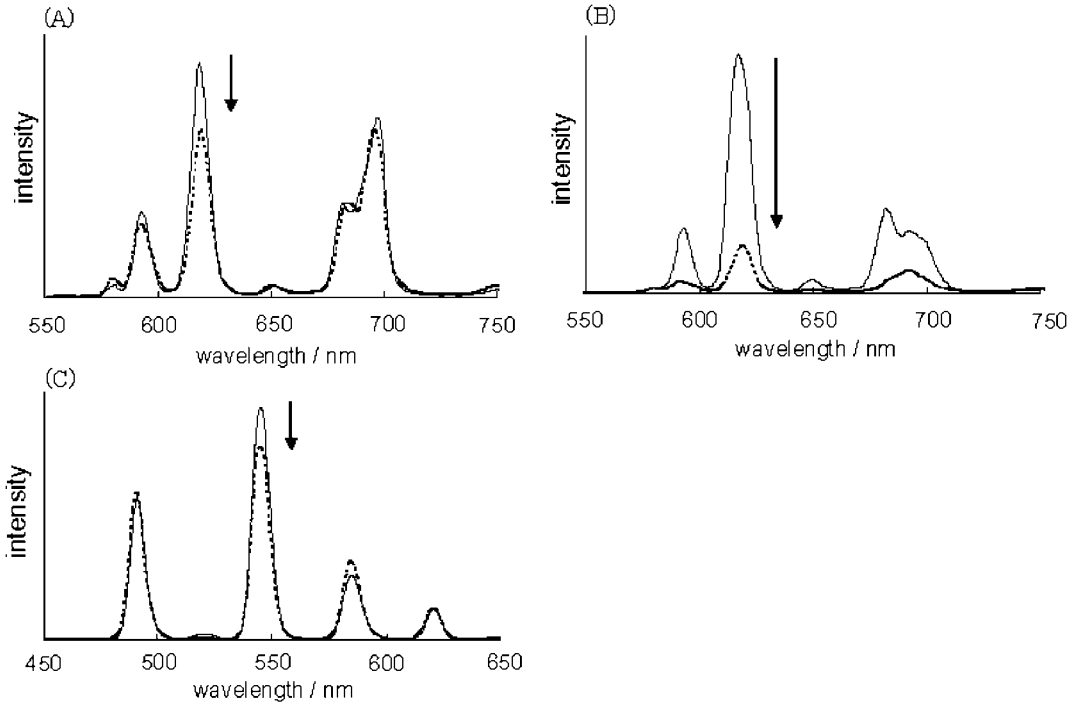

Fig. 7. Emission spectra of [Eu**1**(NO_3)]$(NO_3)_2$ (A), [Eu**2**(NO_3)]$(NO_3)_2$ (B), and [Tb**1**(NO_3)]$(NO_3)_2$ (C) in CH_3CN (solid line) and H_2O (dashed line). The concentration of the complexes was 1.0×10^{-4} mol dm^{-3}.

Table 6. Luminescence Lifetimes and Derived Hydration States of [Eu**1**(NO_3)]$(NO_3)_2$, [Eu**2**(NO_3)]$(NO_3)_2$, and [Tb**1**(NO_3)]$(NO_3)_2$

	τ H_2O/ms	τ D_2O/ms	q H_2O
[Eu**1**(NO_3)]$(NO_3)_2$	0.67	1.28	0.4
[Eu**2**(NO_3)]$(NO_3)_2$	0.25	1.77	3.4
[Tb**1**(NO_3)]$(NO_3)_2$	1.33	1.54	0.2

coordination to the Eu^{3+} and Tb^{3+} complexes was affected by the rigidity of the ligand backbone structure, which also strongly influenced the intensity of their luminescence in water. These findings showed that by controlling the coordination environments with changing the ligand structure, lanthanide complexes with more intense luminescence can be prepared.

Experimental

General. ^{1}H and ^{13}C NMR spectra were recorded on JEOL EX270, AL-400, or Bruker DRX-500 spectrometers. IR spectra and mass spectra were measured with a JASCO FT/IR-620 spectrometer and a SHIMADZU AXIMA-CFR spectrometer, respectively. The recycling of preparative HPLC was performed on a JAI LC-918 (column, JAIGEL-ODS; detector, RI Detector RI-50 and UV Detector RI-50 monitoring at 254 nm). Elemental analysis of the products was performed on a Yanaco MT-6 Type at the Elemental Analysis Center of the University of Tokyo. Water (>18.2 MΩ) was purified with a Millipore system. Other solvents and starting materials were purchased from Aldrich, Kanto Chemicals, or Wako Chemicals and used without further purification.

Synthesis. 1,4,7,10-Tetrakis(2′-pyridylmethyl)-1,4,7,10-tetraazacyclododecane (1): 2-(Chloromethyl)pyridine hydrochloride (0.98 g, 6 mmol) in water (10 mL) was neutralized by slow addition of a 4 M NaOH aqueous solution (ca. 2 mL). To this solution, 1,4,7,10-tetraazacyclododecane tetrahydrochloride (0.32 g, 1 mmol) was slowly added. The reaction mixture was stirred at room temperature for 4 days, and the pH of the mixture was maintained between 7 and 9 by periodic dropwise addition of 4 M NaOH aq. The precipitate was collected by filtration. The product was dissolved in $CHCl_3$ and washed with H_2O to remove Na^+ ions. The solvent was evaporated under a reduced pressure and dried in vacuo. Recrystallization from methanol/ethyl acetate gave an analytically pure compound **1** as colorless cubes (0.11 g, 20%). ^{1}H NMR ($CDCl_3$, 400 MHz): δ 8.47 (d, $J = 4.0$ Hz, 4H), 7.70 (d, $J = 7.3$ Hz, 4H), 7.42 (t, $J = 7.0$ Hz, 4H), 7.09 (t, $J = 5.8$ Hz, 4H), 3.64 (s, 8H), 2.78 (s, 16H). ^{13}C NMR ($CDCl_3$, 125 MHz): δ 160.6, 149.1, 136.4, 123.1, 121.9, 62.0, 53.8. IR (KBr) 2796, 1590, 1567, 1474, 1431, 1366, 1310, 1076, 1048, 989, 755 cm^{-1}. EI-MS: $m/z = 536$ (M^+). Anal. Calcd for $C_{32}H_{40}N_8$: C, 71.61; H, 7.51; N, 20.88%. Found: C, 71.75; H, 7.50; N, 20.84%.

***N*,*N*′,*N*″,*N*‴-Pentakis(2′-pyridylmethyl)diethylenetriamine (2):** 2-(Chloromethyl)pyridine hydrochloride (2.46 g, 15 mmol) in water (10 mL) was neutralized by the slow addition of a 4 M NaOH aqueous solution (ca. 4 mL). To this solution, diethylenetriamine (0.21 g, 2 mmol) was slowly added. The reaction mixture was stirred at room temperature for 4 days, and the pH of the mixture was maintained between 7 and 9 by periodic dropwise addition of 4 M NaOH aq. Water was added, and the product was extracted with diethyl ether. The combined extracts were washed with brine and dried over Na_2SO_4. The solvent was evaporated under reduced pressure, and the residue was dried in vacuo. The residue was purified by column chromatography in a column packed with basic alumina gel using ethyl acetate as an eluent to give **2** as a brown oil. An analytically pure sample was obtained by preparative HPLC (ODS) using methanol as an eluent (0.47 g, 42%). ^{1}H NMR ($CDCl_3$, 270 MHz): δ 8.47 (d, $J = 4.6$ Hz, 5H), 7.57 (t, $J = 6.4$ Hz, 5H), 7.43 (d, $J = 7.8$ Hz, 5H), 7.10 (t, $J = 7.3$ Hz, 5H), 3.75 (s, 8H), 3.66 (s, 2H), 2.65 (s, 8H). ^{13}C NMR

($CDCl_3$, 125 MHz): δ 159.6 (C_q), 148.9 (CH), 148.8 (CH), 136.4 (CH), 136.3 (CH), 122.8 (CH), 121.9 (CH), 121.8 (CH), 60.7 (CH_2), 52.7 (CH_2), 52.2 (CH_2). IR (neat): 3061, 3009, 2943, 2814, 1590, 1432, 761 cm^{-1}. MALDI-TOF-MS: m/z 558.7 (M^+).

***N*,*N*,*N*′,*N*″,*N*″-Pentakis(2′-pyridylmethyl)dipropylenetriamine (3):** Compound **3** was synthesized in the same manner as **2** using 2-(chloromethyl)pyridine hydrochloride (8.20 g, 50 mmol) and dipropylenetriamine (1.31 g, 10 mmol) and isolated as a brown oil. Yield: 0.94 g, 16%. ^{1}H NMR ($CDCl_3$, 270 MHz): δ 8.43 (d, $J = 5.0$ Hz, 5H), 7.59 (t, $J = 7.6$ Hz, 5H), 7.42 (d, $J = 7.9$ Hz, 5H), 7.11 (t, $J = 5.3$ Hz, 5H), 3.75 (s, 8H), 3.62 (s, 2H), 2.52 (t, $J = 7.3$ Hz, 4H), 2.40 (t, $J = 7.3$ Hz, 4H), 1.80 (m, 4H). ^{13}C NMR ($CDCl_3$, 125 MHz): δ 159.6 (C_q), 148.8 (CH), 148.6 (CH), 136.22 (CH), 136.17 (CH), 122.7 (CH), 121.7 (CH), 121.6 (CH), 60.3 (CH_2), 52.4 (CH_2), 52.2 (CH_2), 24.4 (CH_2). IR (neat): 3052, 3008, 2925, 2820, 1590, 1473, 1433, 760 cm^{-1}. MALDI-TOF-MS: m/z 587.0 (M^+).

[Na1]Cl (4): 2-(Chloromethyl)pyridine hydrochloride (0.98 g, 6 mmol) in water (10 mL) was neutralized by slow addition of a 4 M NaOH aqueous solution (ca. 2 mL). To this solution, 1,4,7,10-tetraazacyclododecane tetrahydrochloride (0.32 g, 1 mmol) was slowly added. The reaction mixture was allowed to stir at room temperature for 4 days, and the pH of the mixture was maintained between 7 and 9 by periodic dropwise addition of 4 M NaOH aq. The precipitate was collected by filtration, washed with hexane, and dried in vacuo to afford **4** (0.17 g, 28%). ^{1}H NMR ($CDCl_3$, 400 MHz): δ 7.64 (t, $J = 7.6$ Hz, 5H), 7.40 (d, $J = 4.9$ Hz, 5H), 7.12 (d, $J = 8.1$ Hz, 5H), 6.97 (t, $J = 5.4$ Hz, 5H), 3.79–2.18 (m, 24H). ^{13}C NMR ($CDCl_3$, 125 MHz): δ 158.5 (C_q), 148.7 (CH), 136.9 (CH), 123.8 (CH), 122.4 (CH), 59.0 (CH_2), 50.6 (CH_2), 49.9 (CH_2). IR (KBr): 3052, 2925, 2813, 1593, 1567, 1473, 1094, 762 cm^{-1}. MALDI-TOF-MS: m/z 536.44 ($[M - NaCl]^+$).

[Eu1(NO$_3$)](NO$_3$)$_2$: Compound **1** (1.0 g, 1.9 mmol) and $Eu(NO_3)_3 \cdot 6H_2O$ (0.83 g, 1.9 mmol) were dissolved in acetonitrile (200 mL), and the solution was refluxed for 3 days under N_2 atmosphere. The resulting solid product was removed by filtration. The solvent was evaporated under reduced pressure and dried in vacuo. Recrystallization from methanol/ethyl acetate gave an analytically pure compound [Eu**1**(NO_3)]$(NO_3)_2$ (0.96 g, 58%) as a white powder. Anal. Calcd for $C_{32}H_{40}EuN_{11}O_9$: C, 43.94; H, 4.61; N, 17.61%. Found: C, 43.76; H, 4.88; N, 17.38%.

[Tb1(NO$_3$)](NO$_3$)$_2$·H$_2$O: [Tb**1**(NO_3)]$(NO_3)_2 \cdot H_2O$ was synthesized in the same manner as [Eu**1**(NO_3)]$(NO_3)_2$ from **1** (0.66 g, 1.23 mmol) and $Tb(NO_3)_3 \cdot 6H_2O$ (0.52 g, 1.16 mmol). Yield: 0.56 g, 54%. Anal. Calcd for $C_{32}H_{42}N_{11}O_{10}Tb$: C, 42.72; H, 4.71; N, 17.13%. Found: C, 43.00; H, 4.98; N, 16.87%.

[Eu1(OTf)](OTf)$_2$·2H$_2$O: Compound **1** (0.10 g, 0.19 mmol) and $Eu(OTf)_3$ (0.11 g, 0.19 mmol) were dissolved in acetonitrile (30 mL), and the solution was refluxed for 3 days under N_2 atmosphere. The resulting solid product was removed by filtration. The solvent was evaporated under reduced pressure, and the residue was dried in vacuo. Recrystallization from acetonitrile/diethyl ether gave analytically pure [Eu**1**(OTf)](OTf)$_2 \cdot 2H_2O$ (0.13 g, 60%) as a white powder. Anal. Calcd for $C_{35}H_{44}EuF_9N_8O_{11}S_3$: C, 35.87; H, 3.78; N, 9.56%. Found: C, 35.70; H, 3.99; N, 9.36%.

[Nd1Cl](OTf)$_2$·H$_2$O: Compound **4** (0.90 g, 1.51 mmol) and $Nd(OTf)_3$ (1.10 g, 1.86 mmol) were dissolved in acetonitrile (200 mL), and the solution was refluxed for 3 days under N_2 atmosphere. The resulting solid product was removed by filtration. The solvent was evaporated from the filtrate under reduced pressure, and the residue was dried in vacuo. Recrystallization from dichloromethane/ethyl acetate gave analytically pure [Nd**1**Cl](OTf)$_2 \cdot H_2O$ (0.94 g, 61%) as white crystals. Anal. Calcd for $C_{34}H_{42}ClF_6N_8NdO_7S_2$: C, 39.55; H, 4.10; N, 10.85%. Found: C, 39.19; H, 4.21; N, 10.61%.

[Eu1Cl](OTf)$_2$: [Eu**1**Cl](OTf)$_2$ was synthesized in the same manner as [Nd**1**Cl](OTf)$_2 \cdot H_2O$ from **4** (0.54 g, 0.91 mmol) and $Eu(OTf)_3$ (0.59 g, 0.98 mmol). Yield: 0.62 g, 67%. Anal. Calcd for $C_{34}H_{40}EuClF_6N_8O_6S_2$: C, 39.95; H, 3.94; N, 10.96%. Found: C, 39.64; H, 4.30; N, 10.44%.

[Tb1Cl](OTf)$_2$: [Tb**1**Cl](OTf)$_2$ was synthesized in the same manner as [Nd**1**Cl](OTf)$_2 \cdot H_2O$ from **4** (1.00 g, 1.69 mmol) and $Tb(OTf)_3$ (1.10 g, 1.8 mmol). Yield: 1.30 g, 75%. Anal. Calcd for $C_{34}H_{40}ClF_6N_8O_6S_2Tb$: C, 39.68; H, 3.92; N, 10.89%. Found: C, 39.21; H, 4.37; N, 10.54%.

[Nd1(OTf)](OTf)$_2$·2H$_2$O: [Nd**1**Cl](OTf)$_2 \cdot H_2O$ (0.16 g, 0.16 mmol) and Ag(OTf) (0.047 g, 0.18 mmol) were dissolved in acetonitrile (50 mL). The solution was stirred for 12 h at room temperature. The resulting solid product was removed by filtration. The solvent was evaporated from the filtrate under reduced pressure, and the residue was dried in vacuo. Recrystallization from acetonitrile/diethyl ether gave analytically pure compound [Nd**1**(OTf)](OTf)$_2 \cdot 2H_2O$ (0.12 g, 64%) as white crystals. Anal. Calcd for $C_{35}H_{44}F_9N_8NdO_{11}S_3$: C, 36.11; H, 3.81; N, 9.63%. Found: C, 36.41; H, 4.35; N, 9.05%.

[Tb1(OTf)](OTf)$_2$·H$_2$O: [Tb**1**(OTf)](OTf)$_2 \cdot H_2O$ was synthesized in the same manner as [Nd**1**(OTf)](OTf)$_2 \cdot 2H_2O$ from [Tb**1**Cl](OTf)$_2$ (0.10 g, 0.097 mmol) and Ag(OTf) (0.025 g, 0.097 mmol). Yield: 0.079 g, 70%. Anal. Calcd for $C_{35}H_{42}F_9N_8O_{10}S_3Tb$: C, 36.21; H, 3.65; N, 9.65%. Found: C, 36.27; H, 3.79; N, 9.35%.

[Eu2(NO$_3$)](NO$_3$)$_2$: To a solution of $Eu(NO_3)_3 \cdot 6H_2O$ (0.77 g, 1.7 mmol) in acetonitrile (190 mL) was added a solution of **2** (0.95 g, 1.7 mmol) in acetonitrile (10 mL) under N_2 atmosphere. The solution was stirred for 24 h at room temperature. The resulting solid product was removed by filtration. The solvent was evaporated from the filtrate under reduced pressure to give analytically pure [Eu**2**(NO_3)]$(NO_3)_2$ (0.92 g, 60%) as a pale yellow powder. Anal. Calcd for $C_{34}H_{38}EuN_{11}O_9$: C, 45.54; H, 4.27; N, 17.18%. Found: C, 45.41; H, 4.52; N, 16.96%.

[Tb2(NO$_3$)](NO$_3$)$_2$: [Tb**2**(NO_3)]$(NO_3)_2$ was synthesized in the same manner as [Eu**2**(NO_3)]$(NO_3)_2$ from **2** (0.37 g, 0.66 mmol) and $Tb(NO_3)_3 \cdot 6H_2O$ (0.30 g, 0.66 mmol). Yield: 0.37 g, 62%. Anal. Calcd for $C_{34}H_{38}TbN_{11}O_9$: C, 45.19; H, 4.24; N, 17.05%. Found: C, 44.98; H, 4.48; N, 17.03%.

[Eu2(OTf)](OTf)$_2$: To a solution of $Eu(OTf)_3$ (1.88 g, 3.1 mmol) in acetonitrile (190 mL) was added a solution of **2** (1.75 g, 3.1 mmol) in acetonitrile (10 mL) under N_2 atmosphere. The solution was stirred for 24 h at room temperature. The resulting solid product was removed by filtration. The solvent was evaporated from the filtrate under reduced pressure, and the residue was dried in vacuo. Recrystallization from dichloromethane/ethyl acetate gave an analytically pure compound [Eu**2**(OTf)](OTf)$_2$ (2.43 g, 68%) as colorless cubes. Anal. Calcd for $C_{37}H_{38}F_9EuN_8O_9S_3$: C, 38.38; H, 3.31; N, 9.68%. Found: C, 38.15; H, 3.50; N, 9.44%.

[La2(OTf)](OTf)$_2$: [La**2**(OTf)](OTf)$_2$ was synthesized in the same manner as [Eu**2**(OTf)](OTf)$_2$ from **2** (0.29 g, 0.52 mmol) and $La(OTf)_3$ (0.30 g, 0.51 mmol). Yield: 0.39 g, 67%. Anal. Calcd for $C_{37}H_{38}F_9LaN_8O_9S_3$: C, 38.82; H, 3.35; N, 9.79%. Found: C, 38.67; H, 3.50; N, 9.60%.

[Pr2(OTf)](OTf)$_2$: [Pr**2**(OTf)](OTf)$_2$ was synthesized in the same manner as [Eu**2**(OTf)](OTf)$_2$ from **2** (0.29 g, 0.52 mmol) and $Pr(OTf)_3$ (0.30 g, 0.51 mmol). Yield: 0.35 g, 59%. Anal. Calcd for

$C_{37}H_{38}F_9N_8O_9PrS_3$: C, 38.75; H, 3.34; N, 9.77%. Found: C, 38.47; H, 3.52; N, 9.50%.

[Nd2(OTf)](OTf)$_2$: [Nd**2**(OTf)](OTf)$_2$ was synthesized in the same manner as [Eu**2**(OTf)](OTf)$_2$ from **2** (1.0 g, 1.79 mmol) and Nd(OTf)$_3$ (1.06 g, 1.79 mmol). Yield: 1.38 g, 67%. Anal. Calcd for $C_{37}H_{38}N_8F_9NdO_9S_3$: C, 38.64; H, 3.33; N, 9.74%. Found: C, 38.42; H, 3.60; N, 9.50%.

[Sm2(OTf)](OTf)$_2$: [Sm**2**(OTf)](OTf)$_2$ was synthesized in the same manner as [Eu**2**(OTf)](OTf)$_2$ from **2** (0.28 g, 0.50 mmol) and Sm(OTf)$_3$ (0.30 g, 0.50 mmol). Yield: 0.37 g, 64%. Anal. Calcd for $C_{37}H_{38}F_9N_8O_9S_3Sm$: C, 38.43; H, 3.31; N, 9.69%. Found: C, 38.21; H, 3.57; N, 9.43%.

[Tb2(OTf)](OTf)$_2$·3H$_2$O: [Tb**2**(OTf)](OTf)$_2$·3H$_2$O was synthesized in the same manner as [Eu**2**(OTf)](OTf)$_2$ from **2** (1.0 g, 1.79 mmol) and Tb(OTf)$_3$ (1.08 g, 1.78 mmol). Yield: 1.33 g, 61%. Anal. Calcd for $C_{37}H_{44}F_9N_8O_{12}S_3Tb$: C, 36.46; H, 3.64; N, 9.19%. Found: C, 36.41; H, 3.64; N, 9.02%.

[Eu3(NO$_3$)](NO$_3$)$_2$: [Eu**3**(NO$_3$)](NO$_3$)$_2$ was synthesized in the same manner as [Eu**2**(NO$_3$)](NO$_3$)$_2$ from **3** (1.03 g, 1.76 mmol) and Eu(NO$_3$)$_3$·6H$_2$O (0.79 g, 1.77 mmol). Yield: 1.26 g, 77%. Anal. Calcd for $C_{36}H_{42}EuN_{11}O_9$: C, 46.76; H, 4.58; N, 16.66%. Found: C, 46.58; H, 4.81; N, 16.44%.

[Eu3(OTf)](OTf)$_2$·H$_2$O: To a solution of Eu(OTf)$_3$ (0.038 g, 0.063 mmol) in acetonitrile (45 mL) was added a solution of **3** (0.037 g, 0.063 mmol) in acetonitrile (5 mL) under N_2 atmosphere. The solution was stirred for 24 h at room temperature. The resulting solid product was removed by filtration. The solvent was evaporated from the filtrate under reduced pressure, and the residue was dried in vacuo. Recrystallization from acetonitrile/diethyl ether gave analytically pure [Eu**3**(OTf)](OTf)$_2$·H$_2$O (0.050 g, 81%) as colorless cubes. Anal. Calcd for $C_{39}H_{44}EuF_9N_8O_{10}S_3$: C, 38.91; H, 3.68; N, 9.31%. Found: C, 38.82; H, 4.13; N, 8.90%.

X-ray Crystallography. All crystals were mounted on a loop fiber with liquid paraffin frozen under a cold stream of N_2. Reflection data were collected at 113(2) K on a Rigaku Mercury diffractometer with a CCD area detector or Rigaku VariMax Saturn with graphite monochromated Mo Kα radiation (0.7107 Å). Reflections were corrected for Lorentz and polarization effects, and an empirical correction was applied for absorption. All the structures were solved by direct methods using SIR92 and SHELXS-97.[50,51] The final cycles of full-matrix least-squares refinement on F were performed using the SHELXL-97.[52] All calculations were performed using the CrystalStructure crystallographic software package of Rigaku Corporation or the WinGX program.[53] Crystallographic data have been deposited with Cambridge Crystallographic Data Centre: Deposition number CCDC 290933 for [Nd**1**Cl](OTf)$_2$, CCDC 290934 for [Nd**2**(OTf)](OTf)$_2$, CCDC 290935 for [Pr**2**(OTf)](OTf)$_2$, CCDC 290936 for [Sm**2**(OTf)](OTf)$_2$, CCDC 290937 for [Eu**2**(OTf)](OTf)$_2$·2CH$_2$Cl$_2$, CCDC 290938 for [La**2**(OTf)](OTf)$_2$·2CH$_2$Cl$_2$, CCDC 290939 for [Nd**1**(OTf)](OTf)$_2$·2MeCN·0.5Et$_2$O, CCDC 616549 for [Eu**1**Cl](OTf)$_2$, CCDC 616550 for [Tb**1**Cl](OTf)$_2$, CCDC 616551 for [Eu**1**(OTf)](OTf)$_2$, and CCDC 616552 for [Eu**1**(NO$_3$)](NO$_3$)$_2$. Copies of the data can be obtained free of charge via http://www.ccdc.cam.ac.uk/conts/retrieving.html (or from the Cambridge Crystallographic Data Centre, 12, Union Road, Cambridge, CB2 1EZ, UK; Fax: +44 1223 336033; e-mail: deposit@ccdc.cam.ac.uk).

Luminescence Measurements. The solvents used were distilled water, 99.96% isotopically pure D_2O, and fluorescence-grade acetonitrile. The absorption spectra were recorded with a Jasco V-570 UV–vis spectrometer. The emission and excitation spectra were recorded with a Hitachi FL-4500 spectrometer. The luminescence quantum yields were calculated utilizing the equation $\phi_x/\phi_r = (A_r(\nu)I_r(\nu)n_x^2D_x)/(A_x(\nu)I_x(\nu)n_r^2D_r)$, where x refers to the sample and r to the reference; A is the absorbance, ν the excitation wavenumber, I the intensity of the excitation light at this energy, n the refractive index, and D the integrated emitted intensity. Anthracene was used as a standard ($\phi = 0.27$ in ethanol).[54,55] For the luminescence lifetime study, a pulsed laser was used; Pulsed (10 Hz) 308 nm output of a XeCl excimer laser (Lambda Physik COMPex 201) pumping PBBO (Lambda Physik) was utilized in 1,4-dioxane solution in a dye laser head (Lambda Physik, SCANmate 2). The pulse width was approximately 15 ns. The 355-nm (third harmonic) laser beam was obtained directly from the pulsed (10 Hz) output of a Spectron SL-803 Nd:YAG laser. The emission light was collected, introduced into a monochromator (Oriel 77257), and detected with a photomultiplier tube (Hamamatsu R3896). The signal was picked up with a digitizing oscilloscope (Hewlett Packard 5410A). Obtained decay curves were calculated by a single exponential function and fitted by a least-square method. The resulting decay rate constant k was converted to lifetime τ.

This work was supported by Grants-in-Aid for Scientific Research (Nos. 16047204 (area 434) and 17205007), by a grant from The 21st Century COE Program for Frontiers in Fundamental Chemistry from MEXT, and by CREST, JST, Japan. A. Wada is financially supported by Research Fellowships of Japan Atomic Energy Agency for the Promotion of Science for Young Scientists.

Supporting Information

IR spectra of [Eu**1**(NO$_3$)](NO$_3$)$_2$, [Eu**2**(NO$_3$)](NO$_3$)$_2$, [Eu**3**(NO$_3$)](NO$_3$)$_2$, [Tb**1**(NO$_3$)](NO$_3$)$_2$, and [Tb**2**(NO$_3$)](NO$_3$)$_2$ (Fig. S1). ORTEP drawings of [Nd**1**Cl](OTf)$_2$ (Fig. S2), [Tb**1**Cl](OTf)$_2$ (Fig. S3), [Nd**1**(OTf)](OTf)$_2$ (Fig. S4), [La**2**(OTf)](OTf)$_2$ (Fig. S5), [Pr**2**(OTf)](OTf)$_2$ (Fig. S6), [Nd**2**(OTf)](OTf)$_2$ (Fig. S7), and [Sm**2**(OTf)](OTf)$_2$ (Fig. S8), and the Ln–N bond lengths for [Nd**1**Cl](OTf)$_2$, [Eu**1**Cl](OTf)$_2$, [Tb**1**Cl](OTf)$_2$, [Nd**1**(OTf)](OTf)$_2$, [Eu**1**(OTf)](OTf)$_2$, [Eu**1**(NO$_3$)](NO$_3$)$_2$, [La**2**(OTf)](OTf)$_2$, [Pr**2**(OTf)](OTf)$_2$, [Nd**2**(OTf)](OTf)$_2$, [Sm**2**(OTf)](OTf)$_2$, and [Eu**2**(OTf)](OTf)$_2$ (Table S1). This material is available free of charge on the Web at: http://www.csj.jp/journals/bcsj/.

References

1 D. Parker, J. A. Gareth Williams, *J. Chem. Soc., Dalton Trans.* **1996**, 3613.
2 D. Parker, *Coord. Chem. Rev.* **2000**, *205*, 109.
3 M. P. Lowe, D. Parker, *Inorg. Chim. Acta* **2001**, *317*, 163.
4 J.-C. G. Bünzli, C. Piguet, *Chem. Soc. Rev.* **2005**, *34*, 1048.
5 H. Tsukube, S. Shinoda, *Chem. Rev.* **2002**, *102*, 2389.
6 J. Kido, Y. Okamoto, *Chem. Rev.* **2002**, *102*, 2357.
7 V. W.-W. Yam, K. K.-W. Lo, *Coord. Chem. Rev.* **1999**, *184*, 157.
8 A. K. Saha, K. E. D. Kloszewski, D. A. Upson, J. L. Toner, R. A. Snow, C. D. Black, V. C. Desai, *J. Am. Chem. Soc.* **1993**, *115*, 11032.
9 J. W. Verhoeven, *Pure Appl. Chem.* **1996**, *68*, 2223.
10 J.-C. G. Bünzli, G. R. Choppin, *Lanthanide Probes in Life, Chemical and Earth Sciences*, Elsevier, Amsterdam, **1989**, pp. 219–293.
11 N. Sabbatini, M. Guagliardi, J.-M. Lehn, *Coord. Chem. Rev.* **1993**, *123*, 201.

12 N. Sabbatini, M. Guagliardi, I. Manet, *Handbook on the Physics and Chemistry of Rare Earth*, Elsevier, Amsterdam, **1996**, Vol. 23, pp. 69–119.
13 B. Alpha, R. Ballardini, V. Balzani, J.-M. Lehn, S. Perathoner, N. Sabbatini, *Photochem. Photobiol.* **1990**, *52*, 299.
14 C. Görller-Warland, K. Binnemans, *Handbook on the Physics and Chemistry of Rare Earth*, Elsevier, Amsterdam, **1998**, Vol. 25, pp. 101–264.
15 R. Reusfeld, C. K. Jørgensen, *Laser and Excited States of Rare Earths*, Springer, Berlin, **1977**.
16 J. H. Forsberg, *Coord. Chem. Rev.* **1973**, *10*, 195.
17 B. R. Judd, *Phys. Rev.* **1962**, *127*, 750.
18 G. S. Ofelt, *J. Chem. Phys.* **1962**, *37*, 511.
19 S. Tanabe, T. Hanada, *J. Appl. Phys.* **1994**, *76*, 3730; S. Tanabe, T. Ohyagi, N. Soga, T. Hanada, *Phys. Rev. B* **1992**, *46*, 3305.
20 M. Montalti, L. Prodi, N. Zaccheroni, L. Charbonnière, L. Douce, R. Ziessel, *J. Am. Chem. Soc.* **2001**, *123*, 12694.
21 B. Alpha, J.-M. Lehn, G. Mathis, *Angew. Chem., Int. Ed. Engl.* **1987**, *26*, 266.
22 B. Alpha, V. Balzani, J.-M. Lehn, S. Perathoner, N. Sabbatini, *Angew. Chem., Int. Ed. Engl.* **1987**, *26*, 1266.
23 L. Prodi, M. Maestri, R. Ziessel, V. Balzani, *Inorg. Chem.* **1991**, *30*, 3798.
24 H. Tsukube, Y. Mizutani, S. Shinoda, T. Okazaki, M. Tadokoro, K. Hori, *Inorg. Chem.* **1999**, *38*, 3506.
25 X.-P. Yang, C.-Y. Su, B.-S. Kang, X.-L. Feng, W.-L. Xiao, H.-Q. Liu, *J. Chem. Soc., Dalton Trans.* **2000**, 3253.
26 W. T. Carnall, S. Siegel, J. R. Ferraro, B. Tani, E. Gebert, *Inorg. Chem.* **1973**, *12*, 560.
27 M. Watanabe, T. Nankawa, T. Yamada, T. Kimura, K. Namiki, M. Murata, H. Nishihara, S. Tachimori, *Inorg. Chem.* **2003**, *42*, 6977.
28 V. Alexander, *Chem. Rev.* **1995**, *95*, 273.
29 P. Caravan, J. J. Ellison, T. J. McMury, R. B. Lauffer, *Chem. Rev.* **1999**, *99*, 2293.
30 L. J. Guggenberger, E. L. Muetterties, *J. Am. Chem. Soc.* **1976**, *98*, 7221.
31 L. Jin, R. Wang, L. Li, S. Lu, S. Huang, *Polyhedron* **1998**, *18*, 487.
32 J. Linpei, L. Shuangxi, L. Shaozhe, *Polyhedron* **1996**, *15*, 4069.
33 L. Thompson, J. Legendziewicz, J. Cybinska, L. Pan, W. Brennessel, *J. Alloys Compd.* **2002**, *341*, 312.
34 S. A. Cotton, O. E. Noy, F. Liesener, P. R. Raithby, *Inorg. Chim. Acta* **2003**, *344*, 37.
35 R.-F. Wang, S.-P. Wang, J.-J. Zhang, *J. Mol. Struct.* **2003**, *648*, 151.
36 J.-G. Kang, T.-J. Kim, H.-J. Kang, S. K. Kang, *J. Photochem. Photobiol.* **2005**, *174*, 28.
37 X.-J. Zheng, L.-P. Jin, Z.-M. Wang, C.-H. Yan, S.-Z. Lu, Q. Li, *Polyhedron* **2003**, *22*, 323.
38 B.-L. An, M.-L. Gong, J.-M. Zhang, S.-L. Zheng, *Polyhedron* **2003**, *22*, 2719.
39 J.-G. Kang, M.-K. Na, S.-K. Yoon, Y. Sohn, Y.-D. Kim, I.-H. Suh, *Inorg. Chim. Acta* **2000**, *310*, 56.
40 K. K. Fonda, D. L. Smailes, L. M. Vallarino, G. Bombieri, F. Benetollo, A. Polo, L. de Cola, *Polyhedron* **1993**, *12*, 549.
41 L. Natrajan, J. Pecaut, M. Mazzanti, C. LeBrun, *Inorg. Chem.* **2005**, *44*, 4756.
42 C. R. De Silva, J. Wang, M. D. Carducci, S. A. Rajapakshe, Z. Zheng, *Inorg. Chim. Acta* **2004**, *357*, 630.
43 R. D. Shannon, *Acta Crystallogr., Sect. A* **1976**, *32*, 751.
44 Y. Hasegawa, M. Yamamuro, Y. Wada, N. Kanehisa, Y. Kai, S. Yanagida, *J. Phys. Chem. A* **2003**, *107*, 1697.
45 K. Nakamura, Y. Hasegawa, Y. Wada, S. Yanagida, *Chem. Phys. Lett.* **2004**, *398*, 500.
46 K. Binnemans, R. V. Deun, C. Görller-Warland, S. R. Collinson, F. Martin, D. W. Bruce, C. Wickleder, *Phys. Chem. Chem. Phys.* **2000**, *2*, 3753.
47 A. Beeby, L. M. Bushby, D. Maffeo, G. Williams, *J. Chem. Soc., Dalton Trans.* **2002**, 48.
48 W. D. Horrocks, D. R. Sudnick, *J. Am. Chem. Soc.* **1979**, *101*, 334; R. M. Supkowski, W. D. Horrocks, *Inorg. Chim. Acta* **2002**, *340*, 44.
49 A. Beeby, I. M. Clarkson, R. S. Dickins, S. Faulkner, D. Parker, L. Royle, A. S. Sousa, J. A. G. Williams, M. Woods, *J. Chem. Soc., Perkin Trans. 2* **1999**, 493.
50 A. Altomare, G. Cascarano, C. Giacovazzo, A. Guagliardi, M. C. Burla, G. Polidori, M. Camalli, *J. Appl. Crystallogr.* **1994**, *27*, 435.
51 G. M. Sheldrick, *SHELXS-97, Program for the Solution of Crystal Structures*, University of Göttingen, Germany, **1997**.
52 G. M. Sheldrick, *SHLELXL-97, Program for the Refinement of Crystal Structures*, University of Göttingen, Göttingen, Germany, **1997**.
53 L. J. Farrugia, *J. Appl. Crystallogr.* **1999**, *32*, 837.
54 W. H. Melhuish, *J. Phys. Chem.* **1961**, *65*, 229.
55 G. A. Crosby, J. N. Demas, *J. Phys. Chem.* **1971**, *75*, 991.